Electronic and structural properties of germania polymorphs

Diane M. Christie and James R. Chelikowsky
Department of Chemical Engineering and Materials Science, Minnesota Supercomputer Institute, University of Minnesota, Minneapolis, Minnesota 55455

(Received 25 April 2000; revised manuscript received 17 July 2000)

We present calculations for the electronic and structural properties of three polymorphs of GeO_2: the quartz, rutile, and coesite structures. The last structure is hypothetical. Although germania is not known to exist in the coesite structure, silica does. For this reason, we also include calculations for silica in the coesite structure to facilitate comparisons between the two oxides. Our calculations were performed within the pseudopotential density functional method, i.e., we used pseudopotentials constructed within the local density approximation and a plane wave basis. We determined the lattice parameters, cohesive energy, and bulk modulus by minimizing the total electronic energy of the solid. We find agreement for the structural properties within a few percent of experiment. The calculated electronic band structure, partial density, and total density of states are also presented. We find that for germania, in contrast to silica, the rutile structure is the lowest-energy polymorph.

I. INTRODUCTION

Although GeO_2 is similar to SiO_2, it has not been the subject of extensive studies as has silica. In part, this is due to the great technological importance of silica relative to germania. In addition, silica occurs in many different forms whereas germania does not. As such, silica presents strong theoretical challenges in terms of predicting enthalpies and other thermodynamic properties. At ambient temperature and pressure, the ground state structure for silica is α-quartz (q-SiO_2). Under a pressure above 2 GPa, this form of silica transforms to coesite (c-SiO_2) and to stishovite (r-SiO_2) above 8 GPa. However, it is possible to maintain the quartz structure in a metastable state to about 15 GPa. Above this pressure, the quartz structure transforms to an amorphous state or to a new crystalline state.[1] There also exist a number of high-temperature phases of silica such as crystobalite and trydimite. In contrast, there are only two stable polymorphs of GeO_2 at ambient temperatures: α-quartz (hexagonal) and rutile (tetragonal) structures. GeO_2 rutile corresponds to the stishovite form of SiO_2. The rutile form is hard, colorless, and transparent; it is highly inert and, consequently, may serve as an encapsulating material for germanium semiconductors. The quartz form of germania (q-GeO_2) is interesting from a device standpoint for all the reasons SiO_2 quartz is interesting: It is a hard, transparent, colorless piezoelectric with an index of refraction greater than that of SiO_2 quartz. The rutile structure of germania (r-GeO_2) is stable at ambient temperature and pressure, while the quartz structure is stable above approximately 1300 K at ambient pressure.[2–4] Germania in the quartz structure can be flux grown at a lower temperature and is quenchable to room temperature.[5] Mernagh and Liu demonstrated that q-GeO_2 is the preferred form of germanium oxide at temperatures above 745 K at atmospheric pressure.[6] Since thermodynamic calculations predict that r-GeO_2 should be the stable species under these conditions, they suggest that atmospheric gases (O_2, N_2, H_2O) may have a marked effect on the kinetics and stability of the quartz and rutile forms of GeO_2. A transition from fourfold to sixfold coordination for Ge has been noted when pressure was applied to q-GeO_2.[7] Kinetic studies[8] show a sluggish reaction rate for the transition from quartz to rutile forms for GeO_2 with pressure and temperature. The quartz form of GeO_2 is also transformed irreversibly into an amorphous state at 6–9 GPa.[9] However, no GeO_2 structure corresponding to coesite has been found to exist.

Here, we will investigate the structural and electronic properties of the two existing forms of germanium oxide, quartz and rutile, as well as the hypothetical coesite form (c-GeO_2).

II. COMPUTATIONAL TECHNIQUES

The space groups of q-GeO_2, r-GeO_2, and c-GeO_2 are $P3_121$, $P4_2/mnm$, and $C2/c$, respectively.[10] The structure of q-GeO_2 is hexagonal with three GeO_2 molecules per unit cell. It is characterized by a GeO_4 tetrahedral framework system where a germanium atom is surrounded by four oxygen atoms. It is completely defined by the lattice constants (c,a) and four internal parameters (u,x,y,z). On the other hand, a germanium atom in r-GeO_2 is surrounded by six oxygen atoms in distorted octahedral coordination. This structure is tetragonal with two GeO_2 molecules per unit cell. The unit cell is completely defined by the lattice constants (c,a) and an internal coordinate u. The coesite structure is monoclinic with 16 GeO_2 molecules per conventional unit cell. The primitive cell contains eight GeO_2 molecules and was used for all coesite (c-SiO_2 and c-GeO_2) calculations. The cell is defined by the lattice constants (a,b,c), internal parameters (x,y,z), and angle γ. We fixed γ at 120°. A theoretical determination of the structural parameters involves minimizing a multiparameter total-energy function as a function of the structural parameters. This is the first attempt to our knowledge to use pseudopotentials for calculating the coesite structure for either germania or silica. Coesite is a difficult structure because of the large number of atoms and the large number of degrees of freedom. Since GeO_2 does not occur in the coesite structure whereas SiO_2 does, we

present calculations for SiO_2 coesite in addition to the hypothetical GeO_2 coesite structure.

The electronic and structural properties of germanium oxide were calculated within the framework of the local density approximation (LDA) for which the Kohn-Sham[11,12] equations are solved self-consistently. The exchange and correlation potential of Ceperley and Alder[13] has been used. Previous studies have shown this methodology to yield accurate structural parameters, bulk moduli, and elastic constants for solid state materials.[14–20] Cohesive energies and phase transitions appear to be less well described. For example, Hamann[21] has proposed that a generalized gradient approach[22–24] (GGA) works better for the enthalpies of these systems. However, it is not clear that the GGA is superior to the LDA for other properties. In particular, the compressibility and structural parameters may not be as well described by the GGA. Moreover, most previous work on silica has utilized the LDA. As a first step, we restrict our discussions to LDA calculations.

Our norm-conserving pseudopotentials were constructed to be rapidly convergent with a plane wave basis by the method of Troullier and Martins.[25–27] The pseudopotentials were transformed into the computationally efficient Kleinman-Bylander separable form,[28] using the p component as local for oxygen and the s component as local for germanium to avoid ghost states.[29] The oxygen pseudopotential was generated from the $2s^2 2p^4$ oxygen atomic valence ground state configuration, using a core radius cutoff of 1.79 a.u. for both the s and p pseudopotential components. The nonlocal d component was neglected owing to the high energy of the d state relative to the $2s$ and $2p$ atomic valence states. The germanium pseudopotential was generated from the $4s^2 4p^2 4d^0$ germanium atomic valence ground state configuration, using a core radius cutoff of 2.6 a.u. for the s pseudopotential component, 2.5 a.u. for the p pseudopotential component, and 2.8 a.u. for the d pseudopotential component. For c-SiO_2, the silicon pseudopotential was generated from the $3s^2 3p^2$ silicon atomic valence ground state configuration, using a core radius cutoff of 2.6 a.u. for the s pseudopotential component and 2.7 a.u. for the p pseudopotential component. The Kohn-Sham equation was solved using an iterative diagonalization technique.[26,27,30] Plane waves up to an energy cutoff of 64 Ry were included in the basis set. Typically, about 7000, 3200, and 16 000 plane waves were used in the basis for the quartz, rutile, and coesite structures, respectively. Self-consistency was usually reached in less than 10 iterations with the Fourier components of the potential differing by less than 0.2 mRy from the previous iteration. One special **k** point in the Brillouin zone was used to construct the charge density for self-consistency in the potential for most calculations for the quartz and coesite structures, and six **k** points were used for most calculations for the rutile structure. For the density of states, 13, 18, and 6 **k** points were used for the quartz, rutile, and coesite structures, respectively.

III. EQUATIONS OF STATE

We examined several volumes and determined the optimum internal structure for each polymorph. This was accomplished by minimizing the total energy with respect to the structural parameters for each polymorph, e.g., in the case of coesite we optimize the parameters (a,b,c,u,x,y,z) for each volume.[31] A Murnaghan equation of state[32] was fitted to these points, and was used to determine the equilibrium energy, equilibrium volume, and the bulk modulus.

TABLE I. Bulk modulus of GeO_2 (in GPa). Experimental results for q-GeO_2 are from Refs. 9, 38, 39, 33, and 5. Experimental results for r-GeO_2 are from Refs. 41, 40, 42, and 34. Experimental results for c-SiO_2 are from Refs. 45, 47, 40, 35, 48, and 46.

Structure	Calculated	Experiment
q-GeO_2	37.7	32.8–39.2
r-GeO_2	267	258–395
c-GeO_2	99	(hypothetical)
c-SiO_2	109	93–114

The theoretical result of 38.4 Å^3 for the equilibrium volume of q-GeO_2 underestimates the experimental result[33] of 40.5 Å^3. Calculations for isostructural materials such as SiO_2, $AlPO_4$, and $GaAsO_4$ previously performed by the same method also underestimate the equilibrium volume by ~5% from experiment. Likewise, the calculated result of 24.1 Å^3 for the equilibrium volume of r-GeO_2 underestimates the experimental result[34] of 27.7 Å^3. The theoretical result of 34.0 Å^3 for the equilibrium volume of c-SiO_2 underestimates the experimental result[35] of 34.2 Å^3 by less than 1%. The equilibrium volume of the theoretical form of germania calculated by the same method was found to be 35.2 Å. Assuming the underestimation was approximately the same, this would result in an actual volume of about 35.5 Å^3.

Our value of 6.9 eV/atom for the cohesive energy of q-GeO_2 compares surprisingly well with the experimental value of 6.6 eV/atom.[36] Typically, the LDA overbinds by ~20–30 %. We have included spin-polarization corrections in the cohesive-energy calculation.[37] For germanium the en-

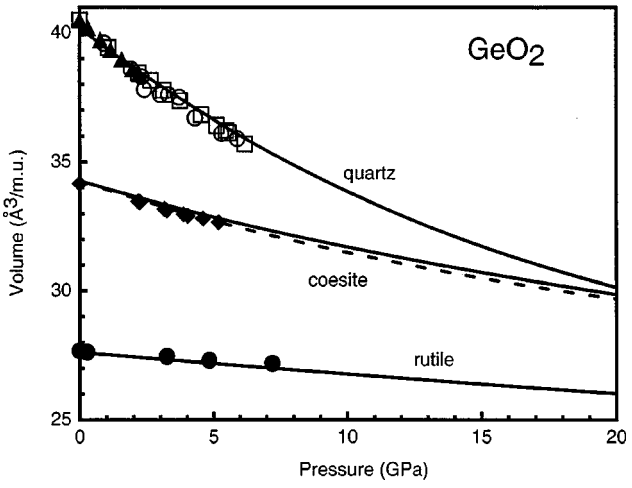

FIG. 1. Equations of state for germanium oxide. Theoretical Murnaghan equation of state fitted from the calculated data points for q-GeO_2, r-GeO_2, and c-GeO_2, respectively. The Murnaghan equation of state for c-SiO_2 (dashed line) is also shown. The experimental data points are from Refs. 5 (open squares), 33 (solid triangles), 9 (open circles), 34 (solid circles), and 35 (solid diamonds).

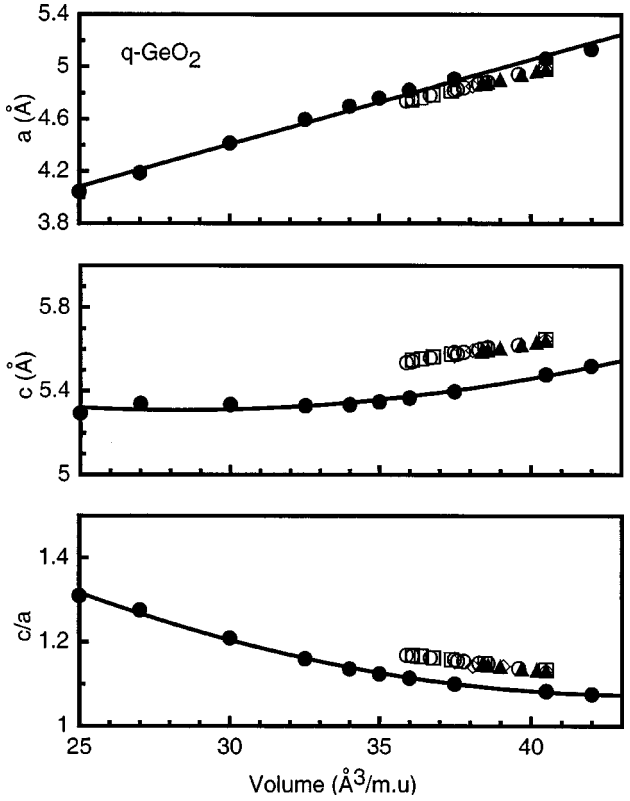

FIG. 2. Theoretical lattice parameters for c, a, and c/a ratio versus the molecular volume for germanium oxide in the quartz structure (q-GeO_2). The experimental data points are from Refs. 5 (open squares), 33 (solid triangles), 9 (open circles), and 34 (open diamonds).

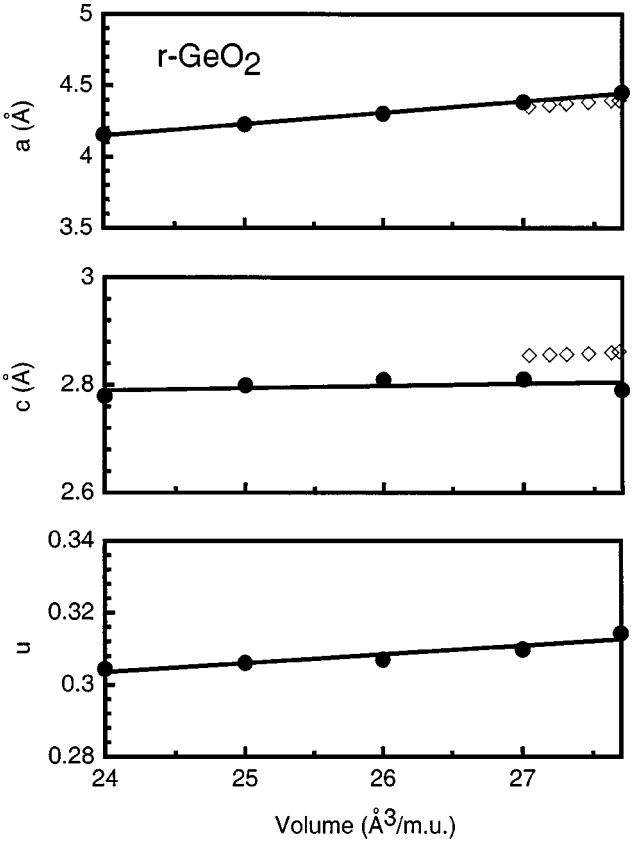

FIG. 3. Theoretical lattice parameters for c, a, and u versus the molecular volume for germanium oxide in the rutile structure (r-GeO_2). The experimental data points are from Ref. 34.

ergy of the pseudoatom is -102.7 eV, including a correction of -2.6 eV for spin polarization. For oxygen the energy of the pseudoatom is -424.9 eV, including a correction of -1.5 eV for spin polarization. To arrive at the experimental binding energy, we used a heat of formation for germania of -131.7 kcal/mol, a cohesive energy for germanium of -90.0 kcal/mol, and a dissociation energy for O_2 of 238.2 kcal/mol.[36] We have not adjusted the experimental values for zero temperature (and zero-point motion). The inherent errors in the local density theory probably exceed any errors present in ignoring the role of temperature. This may not be true for the structural properties; however, we are not in a position at this stage to include changes in structure as a function of temperature. The calculated structural properties are expected to be more accurate than the cohesive energies as the cancellation of errors for the structural properties is expected to be more complete within the local density approximation.

A bulk modulus B_0 of 37.7 GPa was calculated for q-GeO_2 using the *ab initio* pseudopotential method and the Murnaghan equation of state[32]

$$P=\frac{B_0}{B_0'}\left[\left(\frac{V_0}{V}\right)^{B_0'}-1\right], \tag{1}$$

where B_0' was constrained to 4. It is consistent with experimental data shown in Table I where the bulk modulus is found in the range 32.8 to 39.2 GPa. A bulk modulus of 267 GPa was calculated for r-GeO_2 using the same method as we used for q-GeO_2. From Table I, it is seen that the bulk modulus varies greatly from 258 to 395. Our value falls within this range. This is comparable to the isostructural material, stishovite. An experimental[43] bulk modulus of 313 GPa for stishovite has been reported, while the pseudopotential method gave a calculated[44] bulk modulus of 292 GPa. For the coesite structure, a bulk modulus of 109 GPa was calculated for c-SiO_2 using the same method as indicated in previous sections. The theoretical form of germania was found to have a bulk modulus of 99 GPa. From Table I, it is seen that the bulk modulus varies greatly from 93 to 114 GPa for c-SiO_2, and our values for c-SiO_2 and c-GeO_2 fall in this range.

Our volume versus pressure curve (Fig. 1) represents the calculated pressures using Eq. (1) with the theoretical B_0 in Table I. We did not allow B_0' to vary in our fitting procedure owing to the relatively small pressure range over which the Murnaghan expression is expected to be valid. The theoretical Murnaghan equation of state was fitted to the calculated points for q-GeO_2, r-GeO_2, and c-GeO_2. The curve for c-SiO_2 is also shown using a small-dashed line. Our calculations are in good agreement with the experimental data points in Fig. 1. Owing to the good agreement between our calculated and experimental structural parameters for c-SiO_2, we believe the calculated values for c-GeO_2 are likely to be accurately replicated should this structure ever be synthesized.

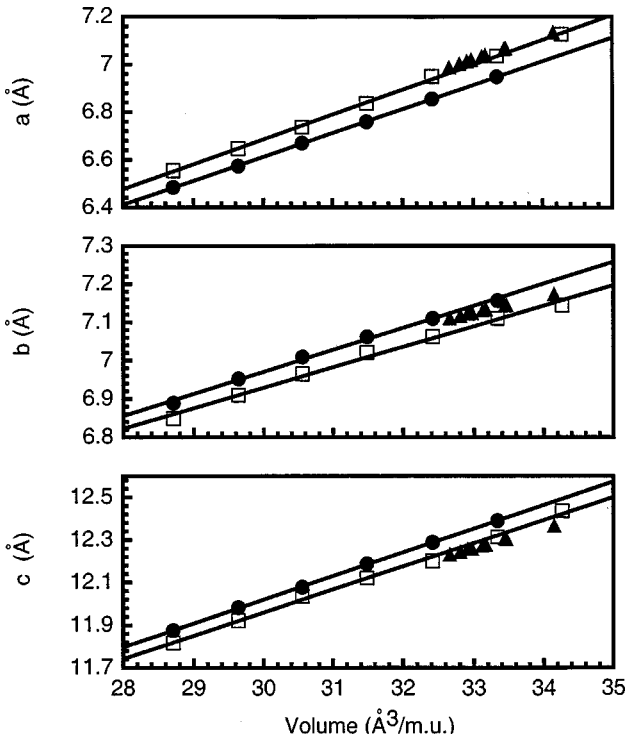

FIG. 4. Theoretical lattice parameters for *a*, *b*, and *c* versus the molecular volume for the hypothetical c-GeO_2 structure (solid circles) and c-SiO_2 (open squares). The experimental data points (solid triangles) are from Ref. 35.

IV. STRUCTURAL PROPERTIES AS A FUNCTION OF PRESSURE

In Fig. 2 we illustrate the (c,a) parameters for q-GeO_2 as a function of volume and compare them to experiment.[5,9,33,34] The *c* and *a* parameters behave in a linear fashion with increasing pressure. The *a* parameter is in almost perfect correlation with experiment, while the *c* parameter varies from experiment by less than 1%. The c/a ratio is also expressed as a near linear function of volume as shown in Fig. 2. Experimentally, this ratio changes by ~4% from 1.13 at ambient pressure to 1.17 at 5.6 GPa (or 36.1 $Å^3$ per molecular unit). Theoretically, the change is also ~3% with the c/a ratio being about 1.08 at ambient pressure and about 1.11 at 36.0 $Å^3$ per molecular unit. The maximum deviation between theoretical and experimental results at any particular pressure is ~5%.

In Fig. 3 we illustrate the *a*, *c*, and *u* parameters as a function of volume for r-GeO_2 and compare them to experiment. The internal parameters vary linearly over a wide pressure regime.

In Fig. 4 we illustrate the *a*, *b*, and *c* parameters for the hypothetical c-GeO_2 structure and c-SiO_2 as a function of volume and compare them to experiment.[35] At room temperature, the crystal is pseudohexagonal with the *a* and *b* parameters approximately equal. As the pressure is increased, the crystal compresses about twice as much in the *a* direction as in the *b* direction. There is a reduction of 4%, 5%, and 8% in the *b*, *c*, and *a* directions, respectively, at a pressure of 28 GPa. In Table II we compare our calculations at ambient pressure to experiment.[35]

TABLE II. Cell dimensions and cell coordinates calculated for the hypothetical c-GeO_2 structure and c-SiO_2 at ambient pressure compared to experimental values determined by Levien and Prewitt (Ref. 35).

	c-GeO_2	c-SiO_2	Experiment
a (Å)	7.0698	7.1267	7.136
b (Å)	7.1912	7.1438	7.174
c (Å)	12.4538	12.4363	12.269
γ	120 (fixed)	120 (fixed)	120.34
Ge/Si(1)	0.1374	0.1417	0.14033
	0.1091	0.1076	0.10833
	0.0725	0.0745	0.07227
Ge/Si(2)	0.5049	0.5071	0.50682
	0.1582	0.1594	0.15799
	0.5422	0.5405	0.54077
O(1)	0.0	0.0	0.0
	0.0	0.0	0.0
	0.0	0.0	0.0
O(2)	0.5	0.5	0.5
	0.1120	0.1205	0.1163
	0.75	0.75	0.75
O(3)	0.2610	0.2708	0.2660
	0.1281	0.1227	0.1234
	0.9364	0.9462	0.9401
O(4)	0.3131	0.3111	0.3114
	0.1022	0.1066	0.1038
	0.3276	0.3288	0.3282
O(5)	0.0256	0.0101	0.0172
	0.2113	0.2117	0.2117
	0.4726	0.4735	0.4782

V. ELECTRONIC STRUCTURE

The total density of states (DOS) for GeO_2 is presented in Fig. 5. The solid, dashed, and dotted lines are q-GeO_2, r-GeO_2, and c-GeO_2, respectively. The valence band maximum is taken as the zero of energy. The density of states was broadened by convoluting with a Gaussian of width equal to 0.5 eV, and the total DOS has been normalized for 48 electrons per unit cell (q-GeO_2), 32 electrons per unit cell (r-GeO_2), and 128 electrons per primitive cell (c-GeO_2).

The total density of states for q-GeO_2 is similar to the density of states of the isomorphic materials silica quartz (SiO_2),[31] berlinite ($AlPO_4$),[20] and gallium arsenate ($GaAsO_4$),[49] as would be expected. The total density of states for r-GeO_2 shows there is no gap at the middle of the valence band separating the bonding from the nonbonding states, unlike in the quartz structure. This is similar to the situation for stishovite (r-SiO_2).[50,51] The total density of states for c-GeO_2 is similar to the density of states of the isomorphic SiO_2 coesite.[51]

The band structure for q-GeO_2 is displayed along the high-symmetry lines in the hexagonal Brillouin zone in Fig. 6. The zero of the energy scale corresponds to the valence band maximum. There are 24 occupied valence bands. The conduction bands within ~10 eV of the valence band maximum are also illustrated. Given the isostructural relationship between germanium oxide, silica quartz,[31] berlinite,[20] and

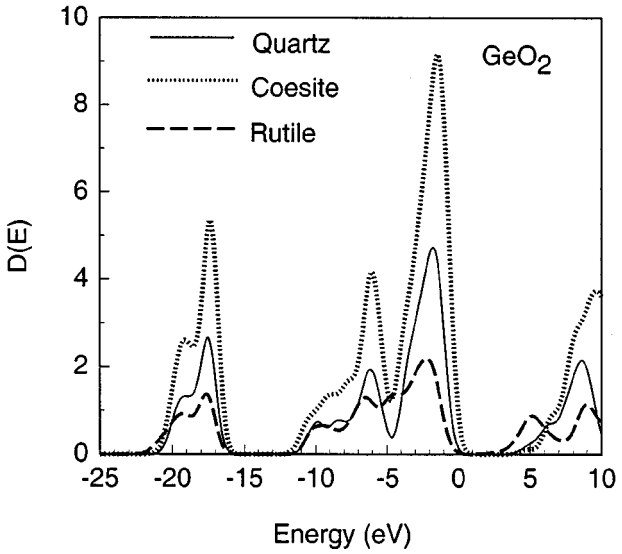

FIG. 5. Total density of states for polymorphs of germanium oxide. The valence band maximum is taken as the zero of energy. The density of states was broadened by convoluting with a Gaussian of width equal to 0.5 eV, and the total DOS has been normalized for 48 electrons per unit cell (q-GeO_2), 32 electrons per unit cell (r-GeO_2), and 128 electrons per primitive cell (c-GeO_2).

gallium arsenate,[49] it is not surprising that the band structures are similar. The theoretical band gap is underestimated owing to the local density approximation. Our calculations yield an indirect band gap for germanium oxide of approximately 5.0 eV from the valence band maximum at K to the conduction band minimum at Γ. The direct band gap at Γ is only

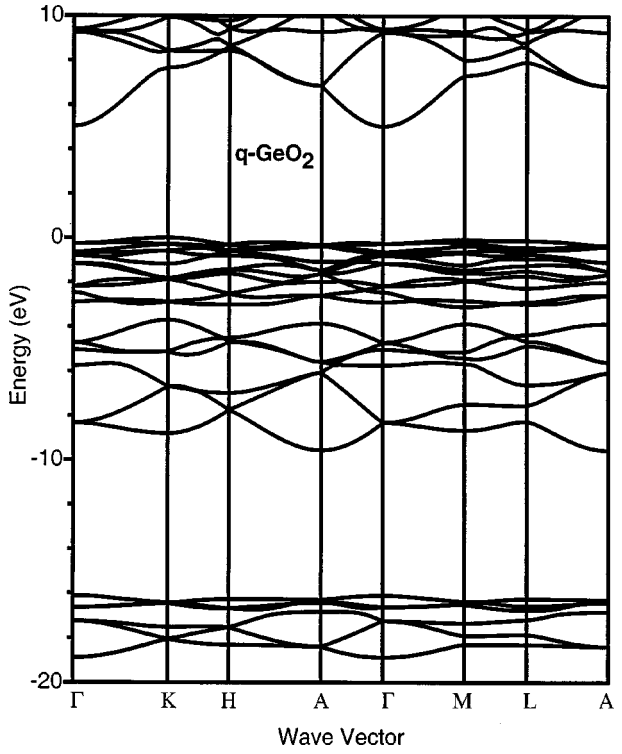

FIG. 6. Electronic band structure of germanium oxide in the quartz structure (q-GeO_2) along high-symmetry directions. The valence band maximum at K is taken as the zero of energy.

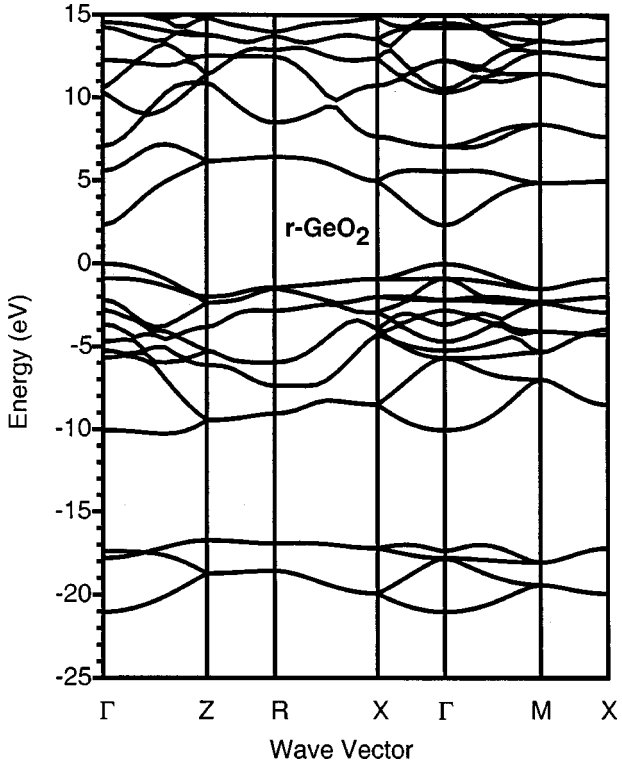

FIG. 7. Electronic band structure of germanium oxide in the rutile structure (r-GeO_2) along high-symmetry directions. The valence band maximum at Γ is taken as the zero of energy.

$\sim$0.1 eV larger than the indirect band gap. This is similar to q-SiO_2 where the LDA gap is also about 5–6 eV and the gap is indirect.[31]

The band structure for r-GeO_2 is displayed along the high-symmetry lines in the tetragonal Brillouin zone in Fig. 7. The zero of the energy scale corresponds to the valence band maximum. There are 16 occupied valence bands. The conduction bands within $\sim$15 eV of the valence band maximum are also illustrated. The band structure is very different from that of the quartz structure, with a wide single valence band rather than two narrow bands. The increased valence bandwidth (due to lack of separation between bonding and nonbonding states) is more metalliclike. GeO_2 looks like SiO_2 under pressure;[52] the band structure is very similar to that of stishovite.[50,51] Our calculations yield a direct band gap at Γ for germanium oxide of approximately 2.4 eV. This LDA gap is probably $\sim\frac{1}{2}$ the true band gap, based on similar comparisons between the LDA and band gaps for quartz.

The structure of coesite is pseudohexagonal. Therefore, the band structure for c-GeO_2 is displayed along the high-symmetry lines in the hexagonal Brillouin zone in Fig. 8. The zero of the energy scale corresponds to the valence band maximum. There are 64 occupied valence bands in the primitive cell. The conduction bands within $\sim$10 eV of the valence band maximum are also illustrated. Our calculations for the theoretical c-GeO_2 structure yield an indirect band gap from the valence band maximum at M to the conduction band minimum at Γ of approximately 5.2 eV. The direct band gap at Γ is only 0.3 eV larger. The band gap for c-SiO_2 has been calculated to be a direct band gap at Γ with estimates of the LDA gap ranging from $\sim$5 to 8 eV.[51,53]

The partial density of states decomposes the density of

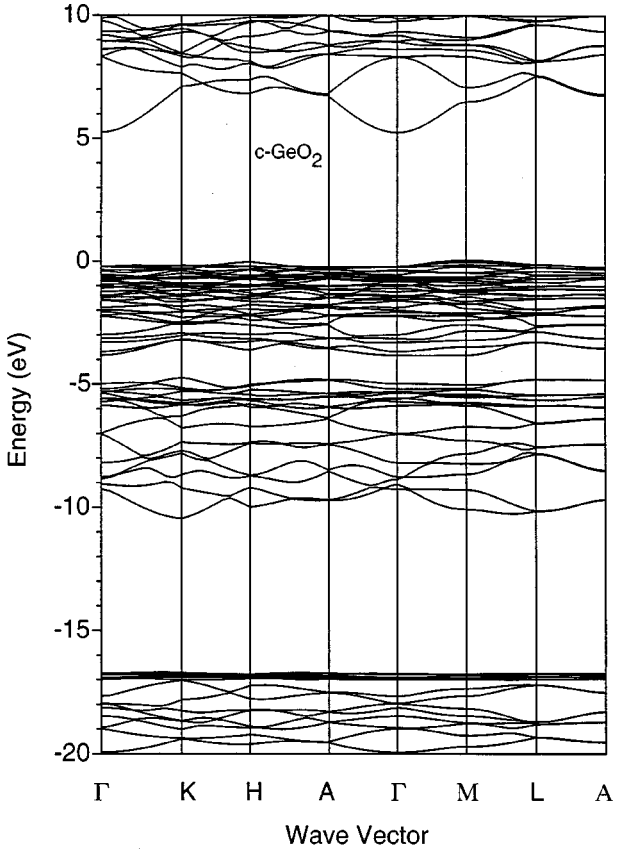

FIG. 8. Electronic band structure of the theoretical c-GeO_2 structure along high-symmetry directions of the pseudohexagonal cell. The valence band maximum at Γ is taken as the zero of energy.

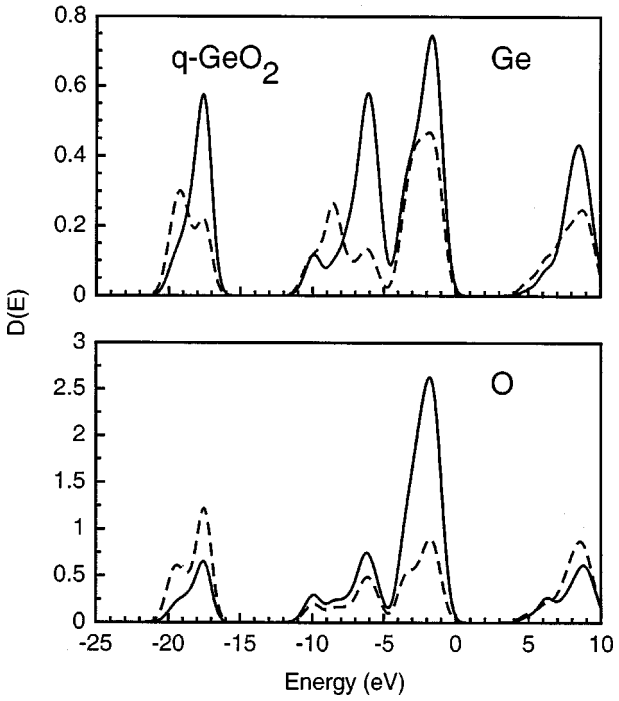

FIG. 9. Partial density of states of germanium oxide in the quartz structure (q-GeO_2). The valence band maximum is taken as the zero of energy. The DOS has been decomposed into the s (dashed line) and p (solid line) angular components. The partial density of states was broadened and normalized as in Fig. 5. Note the change in scale for each atom.

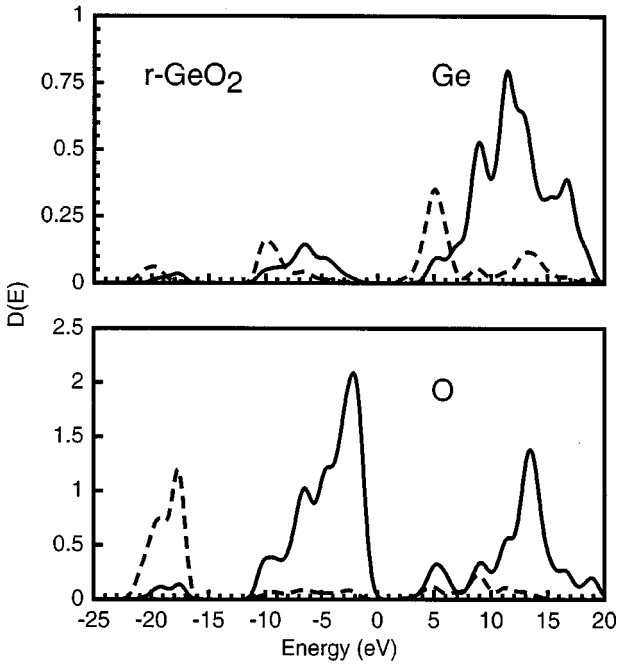

FIG. 10. Partial density of states of germanium oxide in the rutile structure (r-GeO_2). The valence band maximum is taken as the zero of energy. The DOS has been decomposed into the s (dashed line) and p (solid line) angular components. The partial density of states was broadened and normalized as in Fig. 5. Note the change in scale for each decomposition.

states into the s and p angular components associated with a particular atom. The angular momentum decomposition into s and p components was performed using a predetermined radius centered on the atom of interest. The results are somewhat sensitive to the choice of the radius, which is common for this technique. Note the change in scale for each decomposition.

Figure 9 shows that for q-GeO_2 the predominant makeup of the valence band is due to oxygen $(2p)$ states. There are two distinct groups of oxygen $2p$ bands, one from the valence band maximum to ~ -5 eV and a second group from ~ -5 to -11 eV. The higher of the two groups consists mostly of oxygen p lone pair states. The lower group is made up of s and p states occurring in germanium and oxygen, corresponding to bonding states. The radius used for q-GeO_2 was 2.2 a.u.

The partial density of states presented in Fig. 10 was obtained using a radius of 1.95 a.u. centered on the atom of interest. Unlike the tetrahedrally bonded q-GeO_2, there is no gap at the middle of the valence band separating the $O(2p)$ bonding states from the nonbonding states. The predominant makeup of the valence band is due to oxygen $(2p)$ states between -11 and 0 eV, and oxygen $(2s)$ states between -22 and -16 eV.

Figure 11 shows the partial density of states for c-GeO_2 using a radius of 2.1 a.u. The predominant makeup of the valence band is due to oxygen $(2p)$ states. There are two distinct groups of oxygen $2p$ bands, one from the valence band maximum to ~ -5 eV and a second group from ~ -5 to -11 eV. The higher of the two groups consists mostly of oxygen p lone pair states. The lower group is made up of s

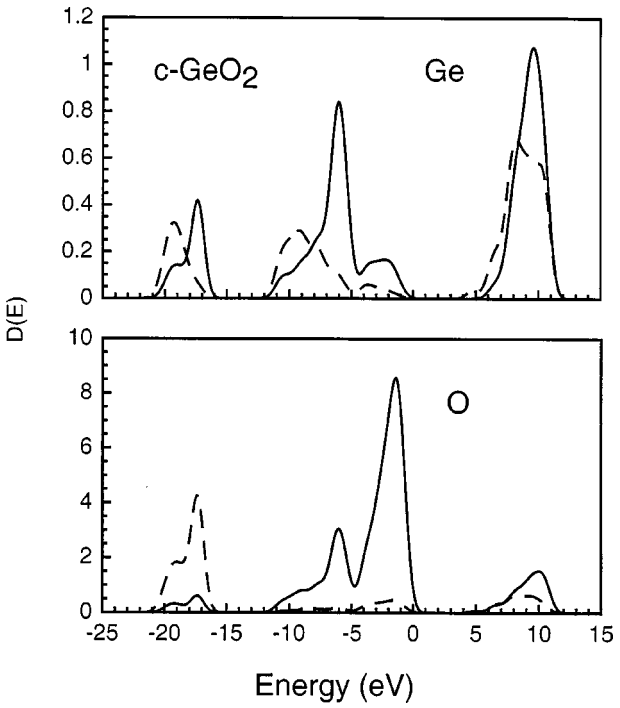

FIG. 11. Partial density of states of the theoretical c-GeO_2 structure. The valence band maximum is taken as the zero of energy. The DOS has been decomposed into the s (dashed line) and p (solid line) angular components. The partial density of states was broadened and normalized as in Fig. 5. Note the change in scale for each decomposition.

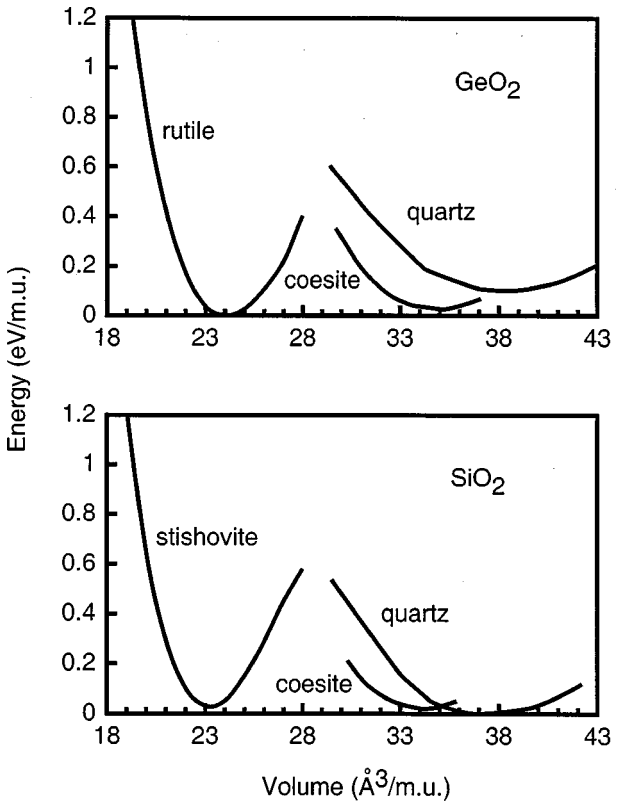

FIG. 12. Total energy per molecular unit as a function of volume for all polymorphs of GeO_2 as compared to the same structures in SiO_2. The zero of the energy scale is rutile for GeO_2 and quartz for SiO_2.

and p states occurring in germanium and oxygen, corresponding to bonding states.

VI. DISCUSSION

We have presented theoretical results for the electronic and structural properties of three polymorphs of germania: two known structures of germania (q-GeO_2 and r-GeO_2) as well as a hypothetical structure (c-GeO_2). We summarize properties for the three structures in Table III. The structural parameters for r-GeO_2 and q-GeO_2 are well replicated by the pseudopotential density functional method, i.e., the structural properties are generally within a few percent of experimental data. Our pressure versus volume curves are also in excellent agreement with experimental data. This is also true for c-SiO_2. The results presented here indicate great similarities between the electronic properties of the coesite structures of SiO_2 and GeO_2. Moreover, the internal coordinates and structural properties of both compounds are very close. Given this similarity, we expect our calculations to determine the properties of a hypothetical c-GeO_2 structure with a reasonable degree of confidence.

We note that the energy difference between r-SiO_2 (stishovite) and q-SiO_2 (quartz) is consistent with previous calculations.[54,55] The experimental difference[56,57] of about 0.5 eV is significantly larger than the 0.03 eV we predicted using the LDA. However, the increasing enthalpy from q-SiO_2 to c-SiO_2 to r-SiO_2 is consistent with silica's transformation behavior under increasing pressure. (See Table IV.)

The total energy per molecular unit versus volume for these three structures in GeO_2 and SiO_2 is shown in Fig. 12. The zero of the energy scales is rutile for GeO_2 and quartz

TABLE III. Comparison of results for germania polymorphs.

	q-GeO_2	c-GeO_2	r-GeO_2
Structure	hexagonal	monoclinic	tetragonal
Molecular units per cell	3	8	2
Equilibrium volume (Å^3/m.u.)	38.4	35.2	24.1
Equilibrium total energy (eV/m.u.)	0.1	0.03	0.0
Bulk modulus (GPa)	37.7	99	267
Electrons	48	128	32
Occupied valence bands	24	64	16
Band gap (eV)	5.0	5.2	2.4

TABLE IV. Comparison of results for silica polymorphs.

	q-SiO_2	c-SiO_2	r-SiO_2
Structure	hexagonal	monoclinic	tetragonal
Molecules	3	8	2
Equilibrium volume (Å^3)	37.0	34.0	23.2
Equilibrium total energy (eV/m.u.)	0.0	0.02	0.03
Bulk modulus (GPa)	37.7	109	278

for SiO_2. As previously noted, it is experimentally unclear[2–9] which species of GeO_2 is ''most stable,'' we find that r-GeO_2 is theoretically the stable species followed by the c-GeO_2 and q-GeO_2 structures. It has also been shown[7,8] that a transition from fourfold to sixfold coordination for Ge occurs when pressure is applied to q-GeO_2, although the reaction rate for the transition to r-GeO_2 was sluggish. Our zero-temperature phase shows notable differences between germania and silica. In germania, we find rutile to be the most stable structure. As such, we predict that q-GeO_2 could transform *without* pressure to c-GeO_2 or to r-GeO_2.

It is interesting to speculate as to why germania would be more stable than silica in the rutile structure. Traditionally, differences between germanium and silicon compounds have focused on the increased metallicity of germanium relative to silicon. For example, GeTe compounds form, as does PbTe, but SiTe does not exist. Thus, one might not be surprised by GeO_2 preferring a structure with a higher oxidation state than the corresponding SiO_2 structure.

While total-energy calculations are quite difficult, we believe the ordering of the polymorphs for germania is correct. In silica, we found that quartz was more stable versus the rutile structure. This is consistent with experiment, but the computed enthalpy difference is larger than that measured. Other density functional approaches such as the generalized gradient approximation have purported to reduce this difference.[21] If this trend is followed in germania, and given the similarities between the systems this is quite probable, then the rutile structure should be stabilized even more than indicated from the LDA calculations.

Our results raise the possibility that either the coesite structure exists, but is yet to be identified, or the hypothetical coesite structure of germania does not form due to other reasons than comparative enthalpies. The fact that only a relatively small number of germania structures have been experimentally identified and characterized is likely a consequence of their existence being controlled by kinetics. We note that Teter *et al.*[58] combined pseudopotential methods with interatomic potentials to model hundreds of hypothetical silica structures with cohesive energies nearly equivalent that of to q-SiO_2. The existence of this myriad of structures is in contrast to what is observed in nature. Silica occurs in only a relatively few structures, principally as q-SiO_2, and to a much lesser extent as cristobalite, tridymite, coesite, and stishovite. Many of these structures are metastable and have only been synthesized in the laboratory. For germania, only r-GeO_2 and q-GeO_2 are known to exist at ambient pressure. We also note that, since r-GeO_2 is found to be lower in energy than q-GeO_2, in contrast to q-SiO_2 and r-SiO_2, it is not clear that the kinetics for silica and germania crystal growth should be similar, i.e., it is not clear that germania will follow the same evolution that leads silica to form the coesite structure.

ACKNOWLEDGMENTS

We would like to acknowledge support for this work by the U.S. Department of Energy under Grant No. DE-FG02-89ER45391, and the Minnesota Supercomputing Institute.

[1] R. M. Wentzcovitch, C. da Silva, J. R. Chelikowsky, and N. Binggeli, Phys. Rev. Lett. **80**, 2149 (1998).
[2] C. B. Clark and G. W. Finch, Am. Mineral. **53**, 1395 (1968).
[3] R. Roy and S. Theokritoff, J. Cryst. Growth **12**, 69 (1972).
[4] L. Liu and W. A. Bassett, *Elements, Oxides and Silicates: High-Pressure Phase Transitions with Implications for the Earth's Mantle* (Oxford University Press, New York, 1986).
[5] J. Glinnemann, H. E. King, Jr., H. Schulz, Th. Hahn, S. J. La Placa, and F. Dacol, Z. Kristallogr. **198**, 177 (1992).
[6] T. P. Mernagh and L. Liu, Phys. Chem. Miner. **24**, 7 (1997).
[7] J. P. Itie, A. Polian, G. Calas, J. Petiau, A. Fontaine, and H. Tolentino, Phys. Rev. Lett. **63**, 398 (1989).
[8] T. Yamanaka, K. Sugiyama, and K. Ogata, J. Appl. Crystallogr. **25**, 11 (1992).
[9] S. Kawasaki, O. Ohtaka, and T. Yamanaka, Phys. Chem. Miner. **20**, 531 (1994).
[10] R. W. G. Wyckoff, *Crystal Structures*, 2nd ed. (Interscience, New York, 1964), Vol. 1, pp. 312–321.
[11] P. Hohenberg and W. Kohn, Phys. Rev. **136**, B864 (1964).
[12] W. Kohn and L. J. Sham, Phys. Rev. **140**, A1133 (1965).
[13] D. M. Ceperley and B. J. Alder, Phys. Rev. Lett. **45**, 566 (1980).
[14] M. T. Yin and M. L. Cohen, Phys. Rev. B **26**, 5668 (1982).
[15] M. T. Yin and M. L. Cohen, Phys. Rev. Lett. **50**, 2006 (1983).
[16] J. R. Chelikowsky and S. G. Louie, Phys. Rev. B **29**, 3470 (1984).
[17] J. R. Chelikowsky, S. G. Louie, D. Vanderbilt, and C. T. Chan, Int. J. Quantum Chem., Symp. **18**, 105 (1984).
[18] J. R. Chelikowsky, C. T. Chan, and S. G. Louie, Phys. Rev. B **34**, 6656 (1986).
[19] K. M. Glassford, N. Troullier, J. L. Martins, and J. R. Chelikowsky, Solid State Commun. **76**, 635 (1990).
[20] D. M. Christie, J. R. Chelikowsky, and N. Troullier, Solid State Commun. **98**, 923 (1996).
[21] D. R. Hamann, Phys. Rev. Lett. **76**, 660 (1996).

[22] J. P. Perdew, J. A. Chevary, S. H. Vosoko, K. A. Jaceson, M. R. Pederson, D. J. Singh, and C. Fiolhais, Phys. Rev. B **46**, 6671 (1992).
[23] A. D. Becke, Phys. Rev. A **38**, 3098 (1988).
[24] A. D. Becke, J. Chem. Phys. **96**, 2155 (1992); J. Andzelm and E. Wimmer, *ibid.* **96**, 1280 (1993).
[25] N. Troullier and J. L. Martins, Solid State Commun. **74**, 613 (1990).
[26] N. Troullier and J. L. Martins, Phys. Rev. B **43**, 1993 (1991).
[27] N. Troullier and J. L. Martins, Phys. Rev. B **43**, 8861 (1991).
[28] L. Kleinman and D. M. Bylander, Phys. Rev. Lett. **48**, 1425 (1982).
[29] X. Gonze, P. Kackell, and M. Scheffler, Phys. Rev. B **41**, 12 264 (1990).
[30] J. L. Martins and M. L. Cohen, Phys. Rev. B **37**, 6134 (1988).
[31] N. Binggeli, N. Troullier, J. L. Martins, and J. R. Chelikowsky, Phys. Rev. B **44**, 4771 (1991).
[32] F. D. Murnaghan, Proc. Natl. Acad. Sci. U.S.A. **3**, 224 (1944).
[33] J. D. Jorgensen, J. Appl. Phys. **49**, 5473 (1978).
[34] T. Yamanaka and K. Ogata, J. Appl. Crystallogr. **24**, 111 (1991).
[35] L. Levien and C. Prewitt, Am. Mineral. **66**, 324 (1981).
[36] *CRC Handbook of Chemistry and Physics*, 64th ed., edited by R. Weast (CRC Press, Boca Raton, FL, 1983).
[37] O. Gunnarsson, B. I. Lundqvist, and J. L. Wilkins, Phys. Rev. B **10**, 1319 (1974).
[38] B. Houser, N. Alberding, R. Ingalls, and E. D. Crozier, Phys. Rev. B **37**, 6513 (1988).
[39] N. Soga, J. Geophys. Res. **76**, 3983 (1971).
[40] R. Liebermann, Phys. Earth Planet. Inter. **7**, 461 (1973).
[41] R. M. Hazen and L. W. Finger, J. Phys. Chem. Solids **42**, 143 (1981).
[42] L. Jolly, B. Silvi, and P. D'Arco, Eur. J. Mineral. **6**, 7 (1994).
[43] M. Sugiyama, S. Endo, and K. Koto, Mineral. J. **13**, 455 (1987).
[44] N. Keskar, N. Troullier, J. L. Martins, and J. R. Chelikowsky, Phys. Rev. B **44**, 4081 (1991).
[45] S. I. Akimoto, Tectonophysics **13**, 161 (1972).
[46] W. A. Bassett and J. D. Barnett, Phys. Earth Planet. Inter. **3**, 54 (1970).
[47] Lin-gun Liu, Mech. Mater. **14**, 283 (1993).
[48] D. J. Weidner and H. R. Carleton, J. Geophys. Res. **82**, 1334 (1977).
[49] D. M. Christie and J. R. Chelikowsky, J. Phys. Chem. Solids **59**, 617 (1998).
[50] J. Alvarez and P. Rez, Solid State Commun. **108**, 37 (1998).
[51] Y.-N. Xu and W. Y. Ching, Phys. Rev. B **44**, 11 048 (1991).
[52] N. Binggeli and J. R. Chelikowsky, Nature (London) **353**, 344 (1991).
[53] Y. P. Li and W. Y. Ching, Phys. Rev. B **31**, 2172 (1985).
[54] N. Keskar and J. R. Chelikowsky, Phys. Rev. B **46**, 1 (1992).
[55] F. Liu, S. H. Garofalini, D. King-Smith, and D. Vanderbilt, Phys. Rev. B **49**, 12 528 (1994).
[56] J. L. Holm, O. J. Kleppa, and E. F. Westrum, Geochim. Cosmochim. Acta **31**, 2289 (1967).
[57] M. Akaogi and A. Navrotsky, Phys. Earth Planet. Inter. **36**, 124 (1984).
[58] D. M. Teter, G. V. Gibbs, M. B. Boisen, D. C. Allan, and M. P. Teter, Phys. Rev. B **52**, 8064 (1995).